Chapter 6

Identification of potential AChE inhibitors through structure-based drug design

6. Identification of potential AChE inhibitors through structure-based drug design

6.1. Introduction

The use of AChE inhibitors is a pivotal for the current symptomatic therapy of AD and are quite successful. Aβ peptide and AChE are reported to be localised in the AD brain [218]. The PAS of AChE acts as an adhesive site to the amyloidogenic conformer of Aβ, leading to its conformational changes and the formation of amyloid fibrils [219]. Thus, designing the PAS binding AChE inhibitor(s) could prevent Aβ aggregation as well as enhance the cholinergic transmission.

In the present study, donepezil and its interactions with AChE were explored to develop a structure-based pharmacophore model. It was employed for the virtual screening of the Zinc15 database. The obtained hits were subjected to various molecular property filters. Further, docking based virtual screening and precision docking were performed to sequentially reduce the number of hits. The prediction of ADMET property and free energy calculations were carried out to obtain three final compounds. Alanine scanning and MD study produced stable complexes of the selected ligands with AChE. The identified compounds would serve as potential leads for AChE inhibition (**Figure 6.1**).

6.2. Material and methods

6.2.1. Pharmacophore hypothesis and database screening using Pharmit

The pharmacophore hypothesis was developed by using the co-crystallized donepezil molecule with AChE (PDB id-4EY7) [220]. The features, i.e. hydrogen bond acceptor, hydrogen bond donor, aromatic groups and hydrophobic centres were used to generate pharmacophore in Ligand Scout 4.1 [221, 222]. The obtained pharmacophore model was used in Pharmit web server (http://pharmit.csb.pitt.edu) [223]. The Zinc15 library, with 123,073,955 conformers of 13,147,339 compounds (accessed on 17-05-2018), was used

to search virtual hits. The search was restricted to one conformer per molecule, and one molecule per hit [196].

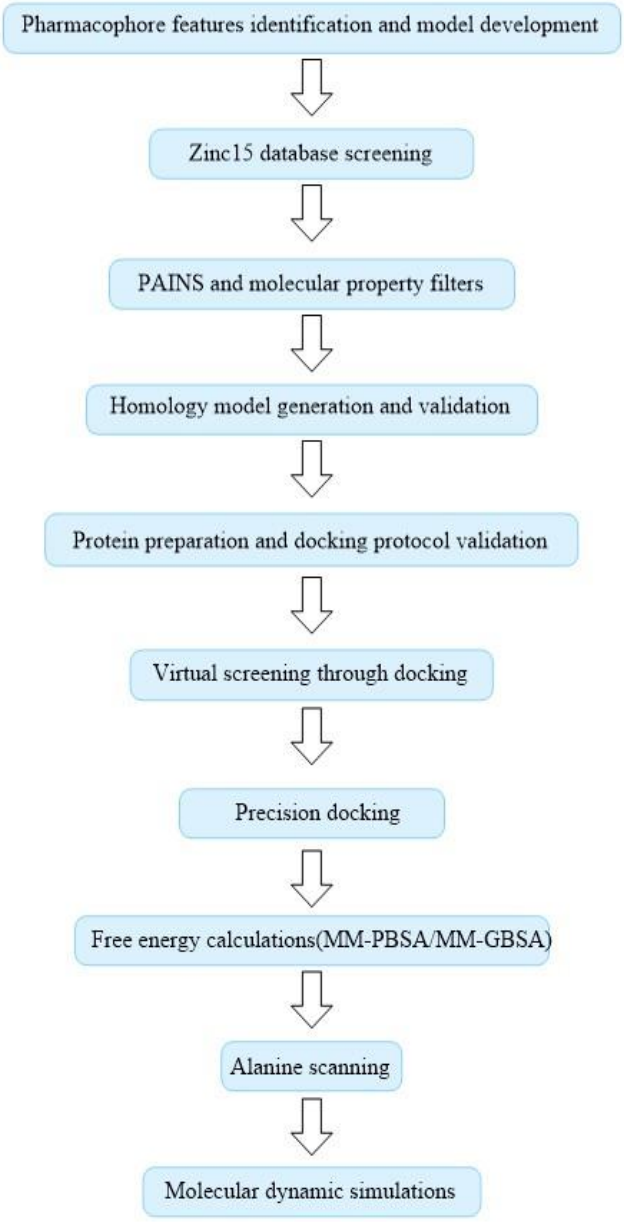

Figure 6.1 Schematic representation of the workflow for *in silico* identification of potential AChE inhibitors.

6.2.2. Molecular property filters

The PAINS were identified using Knime (ver. 3.5.3) using workflow developed by *Saubern et al* [224]. The molecular property filters including molecular weight < 450, logP < 5, H-bond donor < 3, H-bond acceptor < 7, number of rotatable bonds < 8, total number of H-bonds < 8, Pka (neutral or basic) 7.5–10.5 and polar surface area < 70 Å

were also used [225]. The filters were implemented using the Knime workflow to obtain suitable hits [226].

6.2.3. Homology modelling and model validation

The PDB (PDB id: 4EY7) was selected as a protein model for human AChE and was obtained from the protein data bank (https://www.rcsb.org/) [220]. The missing elements were modelled using homology modelling developed by SWISS-MODEL accessible via the ExPASy web server through user template mode [227]. The selected PDB was used as a template, while the target sequence (access code: P22303) was obtained from UniProt (https://www.uniprot.org). Further, the quality of the homology model was evaluated using the PROCHECK [228], RAMPAGE [229], Molprobity [230], GMQE, QMEAN and QMEANDisco [231]. The visualisation of the model was performed with Chimera.

6.2.4. Protein preparation

The PDB2PQR server (http://nbcr-222.ucsd.edu/pdb2pqr_2.1.1) was employed to assign protonation states of amino acid residues of the developed homology model at pH 7.4 using the AMBER force field. Amber ff14SB force field was used to prepare the topology of protein. The AM1-BCC charge scheme was used to assign the atomic charges and General Amber Force Field (GAFF) force field parameters used for donepezil implemented through Antechamber tool. The final coordinate and topology of the complex were built by using *tleap*. The complex was hydrated with TIP3P water using a box size of 89 X 91 X 103 under periodic boundary conditions with 8 Å non-bonded cut-off and Particle Mesh Ewald for the long-range electrostatics. The complex was minimised by an exhaustive protocol including convergence criterion that energy minimisation would halt when RMS reached lower than dmrs, i.e., 1 x 10^{-4} Kcal/mole-Å (**Table T26 in appendix**). It was followed by heating the system for 100 ps to raise the temperature to 310.15 K as the isothermal-isobaric (NPT) ensemble using Langevin

dynamics. Further, the density equilibration and final equilibration were carried out for 100 ps each as an isothermal-isobaric (NPT) ensemble at a temperature of 310.15 K. The final production run of 5 ns was carried out as an isothermal-isobaric (NPT) ensemble at 310.15 K and 1 atm [232, 233]. The last frame of the trajectory of the MD run was converted to PDB and further into pdbqt.

6.2.5. Ligand preparation

The identified hits were subjected to energy minimisation in Open Babel 2.4.0. The ligand was minimized at physiological pH using GAFF with 2500 as maximum steps [234].

6.2.6. Grid generation and validation

Protein-Ligand Interaction Profiler (PLIP) was used to identify the residues involved in non-covalent interactions with donepezil in the selected PDB file. The identified residues were taken as reference points to build a grid box around the active site. The autogrid 4.0 was used to calculate grid maps of interaction energies with various atom types present in the ligands (A, C, HD, NA, N, OA, S, Br, Cl and I). The grid size was set to 74 × 70 × 82 with a grid point spacing of 0.375 Å. Further, the developed grid was validated by redocking donepezil with randomised coordinates. The redocked pose was evaluated by determining RMSD corresponding to the heavy atoms with the co-crystallized structure of donepezil.

6.2.7. Virtual screening and molecular docking

Virtual screening was performed through docking on AutoDock 4.2, which was followed by precision docking of selected compounds. Lamarckian Genetic Algorithm (LGA) was employed for conformational search in both studies. The LGA parameters used for virtual screening and precision dockings are summarised in the table (**Table T27 in appendix)** [188, 235]. The virtual screening results were processed through vstools_v0.16, a python

script. Post-docking analysis and visualisation were performed by Autodock tools 1.5.6 and Discovery Studio visualiser.

6.2.8. ADMET property

The selected compounds were analysed for their absorption, distribution, metabolism, excretion (ADME) properties and carcinogenicity. These properties were predicted through PreADMET server (https://preadmet.bmdrc.kr).

6.2.9. MM-GBSA/MM-PBSA assay

The MM-GBSA and MM-PBSA of the selected compounds were performed using python script, i.e. MMPBSA.py of Amber18 [236]. The MD run for 1 ns was carried using the protocol described in the section 6.2.4. The first 50 frames of obtained trajectories were considered for calculations with a salt concentration of 0.1 mM. The GB model developed by Onufriev *et. al.* was used for MM-GBSA calculations [237]. Further, the total non-polar solvation free energy in MM-PBSA was modelled as linearly proportional to the SASA in a single term. The entropy calculation was neglected in both cases [238].

6.2.10. Alanine scanning

The alanine scanning for the compounds that were selected on the basis of free energy calculations was performed. The residues interacting with the ligands were mutated to alanine, and their contributions to the binding energy of ligands were calculated using the same simulation run as used for free energy calculations. The individual residues were mutated, followed by building the topology and coordinates files of the respective mutated PDBs by *tleap*. The MMGBSA.py, a python script, was used to perform virtual alanine scanning for the first 50 frames of each simulation at a salt concentration of 0.1 mM for both MM-GBSA and MM-PBSA calculations [239].

6.2.11. Molecular dynamics

MD was performed for ACHE, AChE-ZINC000035596918, AChE-ZINC000035551243, and AChE-ZINC000013179534 complexes through Amber18. The protein-ligand complexes were soaked in TIP3P hydrated cubic box with a cut-off distance of 12 Å. The residual charges of the system were neutralised by using counter ions placed in the system. The PME was used to handle long-range electrostatic interactions. The MD systems were subjected to energy minimisation followed by heating, density equilibration, and equilibration under periodic boundary conditions. The detailed experimental protocols are summarised in the tables The final production phase of 50 ns was carried out at 310.15 K as an NPT ensemble (**Table T26** and **T28** in **appendix)** [238].

6.3. Results and discussion

6.3.1. Pharmacophore hypothesis and database screening using Pharmit

Donepezil is a reversible AChE inhibitor producing mixed as well as a non-competitive mode of inhibition with an IC_{50} of 5.7 nM [240]. Ligand scout identified protein-ligand interactions of donepezil with AChE and derived a pharmacophore model with two aromatic rings (A) and four hydrogen bond acceptors (HA) (**Figure 6.2**).

a

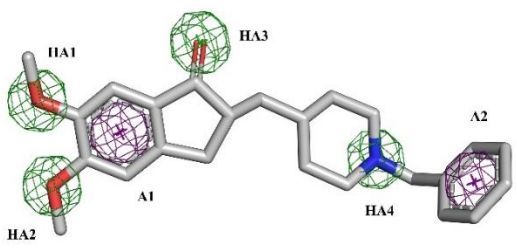

b

A1	0					
A2	11.5	0				
HA1	2.8	14.2	0			
HA2	2.8	13.6	2.7	0		
HA3	3.8	9.7	5.5	6.6	0	
HA4	8.6	3.7	11.3	10.7	7.3	0
	A1	A2	HA1	HA2	HA3	HA4

Figure 6.2 (a) Pharmacophore model developed from co-crystallised donepezil (b) Distance between various pharmacophore features.

The obtained pharmacophore was queried against Zinc15 database, through Pharmit server, to identify the virtual hits. Six hundred one molecules with diverse structures

containing various heterocyclic rings, including thiazoles, benzothiazoles, piperazines, pyrimidines, pyridines, quinazolines, pyrazoles, piperidines etc. were obtained.

6.3.2. Molecular property filters

PAINS compound filtration was performed by using SMARTS pattern search and 571 compounds showed the absence of PAINS SMARTS patterns. The compounds were further subjected to a physicochemical property filter to obtain 199 compounds.

6.3.3. Homology modelling and model validation

The careful inspection of human AChE PDB (PDB id - 4EY7) indicated the absence of residues 259-264 and 495-497. Therefore, a homology model was developed to fill the missing structures using SWISS-MODEL. Ramachandran plot was obtained from two web servers: PROCHECK (https://servicesn.mbi.ucla.edu/procheck) and RAMPAGE (http://mordred.bioc.cam.ac.uk/~rapper/rampage.php) (**Figure 6.3**). The quality of the model was appropriate with more than 90% of residues in the most favoured region (**Table 6.1**). The developed model displayed a MolProbity score of 0.93 indicating the acceptable quality of the model and displayed only a single steric clash between Arg18-Asp61 [241]. GMQE Score for the model was 0.99 indicating the closeness of the model and template. Further, the model had a QMEAN score of 0.88 and favourable torsion angle potential. Hence, the validation parameters indicated confidence over the developed model of human AChE.

Table 6.1 Ramachandran parameter for developed homology model using PROCHECK and RAMPAGE

	Residues in allowed region(%)	**Residues in outlier region(%)**
PROCHECK	99.8	0.2
RAMPAGE	99.7	0.4

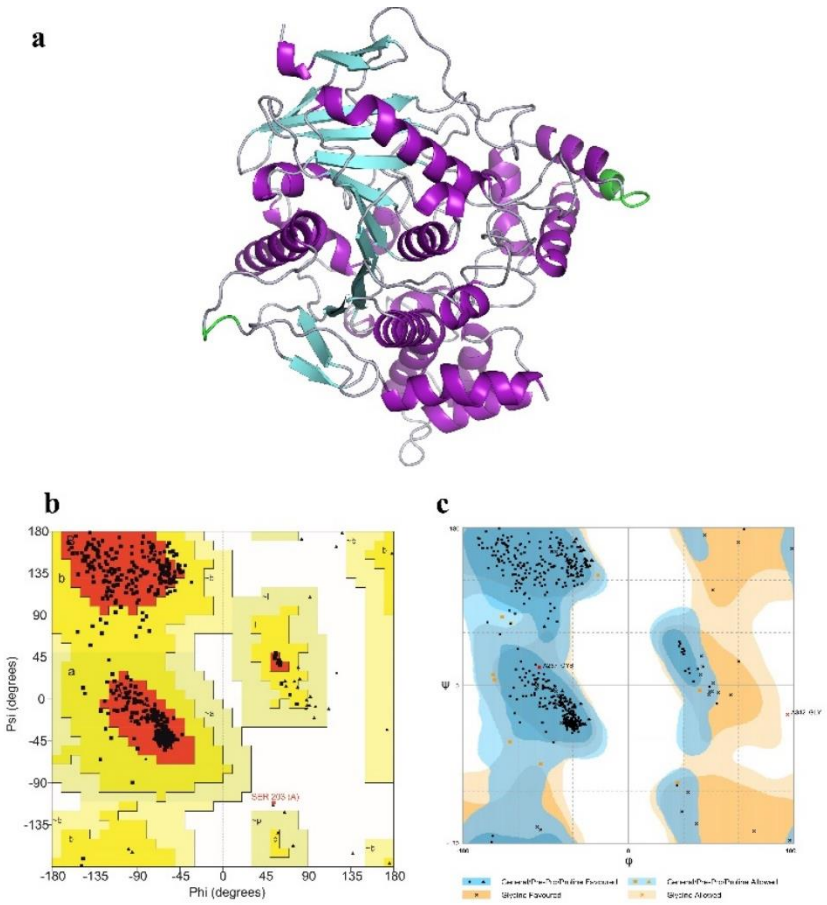

Figure 6.3 (a) Homology model of human AChE with the modelled loops in green. (b & c) Ramachandran plot of the homology model obtained from PROCHECK and RAMPAGE.

6.3.4. Protein preparation

The PDB2PQR server was used to prepare protein structure at physiological pH 7.4. The PROPKA utility was used to assign the correct protonation state to amino acid residues. Proper inclusion of flexibility during protein structure preparation is essential for the success of virtual screening and docking studies. Thus, energy minimisation, heating at 310.15 K, followed by NVT and NPT equilibration and a mini-MD run of 5 ns was performed to enable the side chain of residues to be relaxed and acquire suitable conformation at physiological conditions provided. MD run of 5 ns displayed a steady trajectory with a mean RMSD deviation of 1.412 (**Figure S10 in appendix**). The end frame of the obtained trajectory was converted to PDB and was used to perform virtual screening and molecular docking.

6.3.5. Ligand preparation

The selected compounds were subjected to energy minimisation in order to rectify the geometry, remove the steric clashes and overlapping atoms of the compounds. The local energy minimum was identified using the steepest descent algorithm.

6.3.6. Grid generation and validation

PLIP server was used for the identification of essential interactions of donepezil with protein residues present in the selected PDB. The interactions with a distance of less than 5 Å were selected for the grid generation. Donepezil displayed hydrophobic interactions with Trp86, Tyr337, Phe338, and Tyr341 along with a hydrogen bonding with Phe295. It also showed π-π interactions with Trp86, Trp236, and Tyr34. The grid box dimensions and grid point spacing criteria was genrated using these residues and were validated. The accuracy of docking protocol can be determined by the ability to efficiently reproduce the pose similar to the co-crystallised ligand conformation with least deviation. The selected grid parameters displayed acceptable RMSD deviations of 0.967 and 1.465 Å between re-docked donepezil pose with homology model and MD derived donepezil poses respectively, over 28 pairs of heavy atoms (**Figure 6.4**). Thus, it was inferred that the generated grid would produce reproducible and reliable results [242].

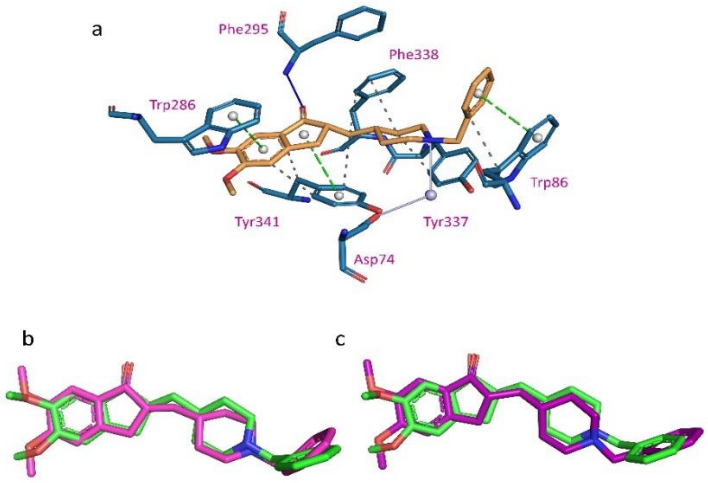

Figure 6.4 (a) Binding site of donepezil inhibiting human AChE (b & c) Superimposition of docked structure (green) with co-crystallised and molecular dynamics generated structure of donepezil (magenta and purple).

6.3.7. Virtual screening and molecular docking

The virtual screening of 198 ligands, we obtained 21 compounds with binding energy ranging from -11.94 to -7.69 kcal/mol. The virtual screening results displayed a near normal distribution in terms of binding energies of compounds with a mean binding energy of -10.41 Kcal/mol. The compounds displaying a cluster size of 6 and above were only considered for precision docking. The precision docking was carried out by using extended LGA parameters with a population size of 100. The cluster size of 50 and above with an RMSD tolerance limit of 2 Å was used to filter the compounds in order to ascertain the binding site of each ligand. Five ligands with a cluster size greater than 50 were selected for further study. The detailed docking results are reported in **Table 6.2**. Compound ZINC000013719534 displayed two hydrogen bond interactions with Phe296 and Arg295. The *naphtho[2,3-d][1,3]dioxol-5(8H)-one* ring of the ligand interacted with Trp286 and Tyr341 through π-π interactions, while Tyr124 interacted with terminal *tolyl* ring. The *N-ethyl* group displayed π-alkyl interactions with Trp286 and Tyr341. Further, the *piperidine* ring interacted with Phe338 and Tyr341 and *naphtho[2,3-d][1,3]dioxol-5(8H)-one* ring with Leu289. Gly122 and Gln291 displayed weak van der Waals interactions. The precision docking of ZINC000169753041 with AChE displayed hydrogen bonding interaction with one of the PAS residues, i.e. Tyr72. The *methoxy* group as well as *pyrazole* hydrogen also formed hydrogen bond interactions with Thr75 and Arg295. The PAS residues Trp286 and Tyr341 interacted with the two divergent *phenyl* rings of the molecule and also with the *pyrazole* ring. Tyr124, Ser293 and Tyr341 formed van der Waals interactions with the ligand. ZINC000035551243 displayed hydrogen-bonding pattern with Trp86. Ser125 formed π-donor hydrogen bond interaction with *benzo[d][1,3]dioxole* ring. Further, Phe297 Phe338 and Tyr341 formed π-alkyl interactions with the ligand. ZINC000035596918 displayed a hydrogen bond with Gly121, Gly122, Tyr124, Glu292, Phe295 and His447. Gly121 displayed π-π stacking

between the *amide* bond of *glycine* and the terminal *phenyl* ring. The residues Val294, Tyr337, Phe338 and Tyr341 of AchE displayed π-alkyl interactions. ZINC000014996252 formed a hydrogen bond with Arg296, Glu292 and Ser293. The *thiophene* ring interacted with Leu289 residue with π-alkyl bonding and Trp286 with terminal *phenyl* ring with π-π interaction (**Figure 6.5**).

Table 6.2 Docking results displaying mean binding energy, cluster size and lowest binding energy of ligands against AChE (PDB id 4EY7).

Compound_code	Mean binding energy *(kcal/mol)	Cluster count	Lowest binding energy (kcal/mol)
ZINC000013719534	-10.97 ± 0.022	98	-11.01
ZINC000169753041	-11.19 ± 0.304	77	-11.68
ZINC000035551243	-10.81 ± 0.033	75	-10.84
ZINC000035596918	-10.66 ± 0.066	60	-10.72
ZINC000014996252	-10.41 ± 0.263	54	-10.76
ZINC000067285335	-10.49 ± 0.352	49	-11.08
ZINC000096269068	-9.26 ± 0.031	48	-9.32
ZINC000020357495	-11.6 ± 0.167	42	-11.89
ZINC000013694979	10.09 ± 0.045	41	-10.15
ZINC000010186527	-9.46 ± 0.060	40	-9.71
ZINC000072347166	-11.62 ± 0.352	37	-11.92
ZINC000007744477	-10.5 ± 0.555	35	-11.45
ZINC000023003047	-9.81 ± 0.337	31	-10.46
ZINC000096324194	-10.28 ± 0.077	29	-10.47
ZINC000008164479	-10.45 ± 0.120	28	-10.55
ZINC000585604788	-11.26 ± 0.194	28	-11.43
ZINC000581797407	-10.21 ± 0.148	23	-10.4
ZINC000009951864	-10.63 ± 0.326	20	-10.95
ZINC000012971535	-9.88 ± 0.018	19	-9.91
ZINC000102830640	-10.78 ± 0.773	14	-11.98
ZINC000045727895	-10.77 ± 0.094	13	-10.94
Donepezil	-11.16 ± 0. 941	78	-10.98

*Data are expressed as Mean ± SD

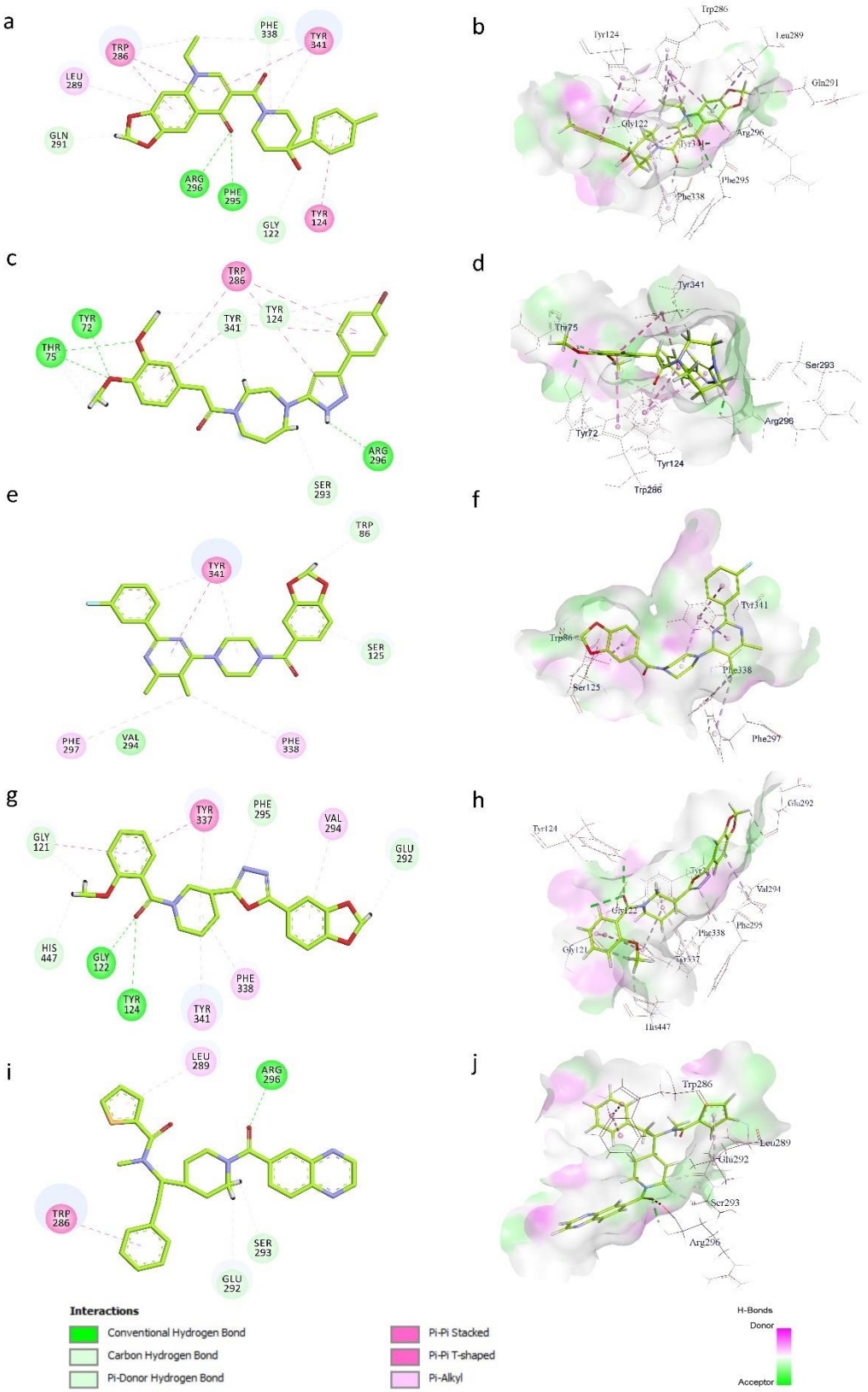

Figure 6.5 2D and 3D interaction diagrams of (a & b) ZINC000169753041, (c & d) ZINC000013719534, (e & f) ZINC000035551243, (g & h) ZINC000035596918, and (i & j) ZINC000014996252.

6.3.8. ADMET property

The absorption of the drug is a limiting factor for its bioavailability and response. The predicted human intestinal absorption (HIA) for all the selected compounds were greater than 95%. ZINC000035596918 displayed a maximum HIA of 99.26 %. The molecules with BB (C_{brain}/C_{blood}) range from 0.1-2.0 indicate moderate BBB penetration. The identified compounds displayed C_{brain}/C_{blood} range of 0.2-0.6, i.e., moderate BBB penetration. The compounds were found to be an inhibitor of CYP2C19 and CYP3A4 and non-substrate of CYP2D6. Further, moderate plasma protein binding was observed in the case of all the selected molecules. The rodent carcinogenicity model based on data of the National Toxicology Program and US FDA of mice and rats for two years was used to predict the carcinogenicity. The selected compounds were found to be non-carcinogenic in rat and mouse (**Table 6.3**).

Table 6.3 Predicted pharmacokinetic properties and toxicity of selected compounds.

Compound_code	BBB	CYP2C19 inhibition	CYP2D6 substrate	CYP3A4 inhibition	HIA	Plasma Protein Binding
ZINC000013719534	0.22	Non	Non	Non	96.5	85.31
ZINC000169753041	0.43	Non	Non	Non	97.74	83.76
ZINC000035551243	0.250	Non	Non	Non	97.65	88.78
ZINC000035596918	0.172	Non	Non	Non	99.26	88.01
ZINC000014996252	0.526	Non	Non	Non	97.75	91.745

6.3.9. MM-GBSA/MM-PBSA assay

The mean ΔG_{MMGBSA} for ZINC000013719534, ZINC000035551243 and ZINC000035596918 was better than Donepezil and similar results were observed in ΔG_{MMPBSA} study (**Table 6.4** and **6.5**). The results of precision docking, however, showed deviation from these results as compound ZINC000169753041 was found to have better binding energy than others, which was not observed in case of both free energy calculations. The reason for the observation might be non-inclusion of the water molecules in the docking, hence, the free energy calculations a superior method for the

calculation of binding energies than the scoring functions that are used to evaluate docking poses.

Table 6.4 Energy contributions of protein-ligand complexes in MM-GBSA assay.

Compound code	ΔE_{vdw}	ΔE_{ele}	ΔG_{GB}	ΔG_{SA}	ΔG_{MMGBSA}
ZINC000013719534	-57.952 ± 0.439	-34.999 ± 0.492	55.684 ± 0.463	-6.557 ± 0.026	-43.824 ± 0.420
ZINC000169753041	-53.762 ± 0.440	-21.382 ± 0.576	42.520 ± 0.434	-5.965 ± 0.038	-38.589 ± 0.493
ZINC000035551243	-61.706 ± 0.579	-19.774 ± 0.624	39.221 ± 0.383	-6.868 ± 0.021	-49.128 ± 0.675
ZINC000035596918	-55.721 ± 0.449	-27.660 ± 0.808	46.178 ± 0.619	-6.263 ± 0.033	-43.467 ± 0.554
ZINC000014996252	-55.889 ± 0.469	-26.848 ± 0.575	53.654 ± 0.486	-6.451 ± 0.036	-35.535 ± 0.388
Donepezil	-53.770 ± 0.414	-15.485 ± 0.474	34.950 ± 0.446	-6.406 ± 0.035	-40.698 ± 0.461

All data are expressed as Mean ± SEM.

Table 6.5 Energy contributions of protein-ligand complexes in MM-PBSA assay.

Compound code	ΔE_{vdw}	ΔE_{ele}	ΔG_{PB}	$\Delta G_{Nonpolar}$	ΔG_{MMPBSA}
ZINC000013719534	-57.952 ± 0.439	-34.999 ± 0.492	64.363 ± 0.614	-4.844 ± 0.017	-33.433 ± 0.525
ZINC000169753041	-53.762 ± 0.44	-21.382 ± 0.576	50.021 ± 0.467	-4.606 ± 0.021	-29.729 ± 0.663
ZINC000035551243	-61.706 ± 0.579	-19.774 ± 0.624	49.037 ± 0.492	-5.047 ± 0.013	-37.490 ± 0.815
ZINC000035596918	-55.721 ± 0.449	-27.660 ± 0.808	54.812 ± 0.075	-4.816 ± 0.017	-33.386 ± 0.668
ZINC000014996252	-55.889 ± 0.469	-26.848 ± 0.575	61.090 ± 0.586	-4.871 ± 0.020	-26.518 ± 0.503
Donepezil	-53.770 ± 0.414	-15.485 ± 0.474	49.891 ± 0.586	-5.087 ± 0.011	-24.437 ± 0.481

All data are expressed as Mean ± SEM.

6.3.10. Alanine scanning

In this study, the virtual alanine scanning for three compounds, i.e. ZINC000013719534, ZINC000035551243 and ZINC000035596918.was performed. The alanine scanning for ZINC000013719534 displayed that Trp286 and Tyr341 played a pivotal role in its binding due to higher losses in the binding energy of -4.78 and -4.49 in case of MM-GBSA and -3.82 and -2.46 in case of MM-PBSA respectively. The docking pose also reflected similar results, as both residues displayed π-π and π-alkyl interactions with the ligand. Tyr124

(π-π) and Phe338 (π-alkyl) residues displayed the next significant contribution. Further, the Arg296 was also significantly contributing towards free binding energies.

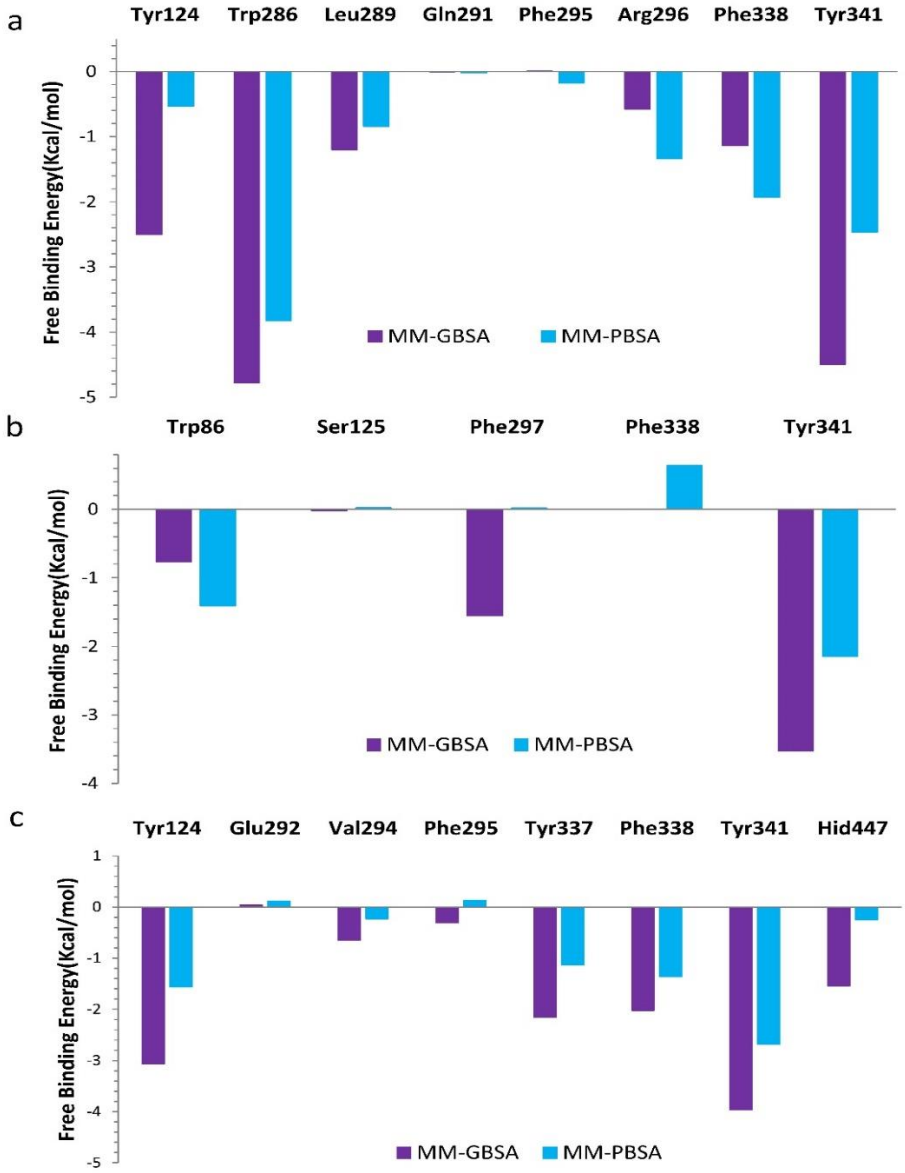

Figure 6.6 Virtual alanine scanning analysis of critical interacting residues of compounds (a) ZINC000013719534, (b) ZINC000035551243 and (c) ZINC000035596918

A virtual alanine study of ZINC000035551243 revealed the two crucial interactions with AS and PAS residues, i.e., Trp86 and Tyr341, respectively. Further, the docking study also displayed that the binding of the ligand was much contributed by van der Waals interactions with Gln71, Tyr72, Asp74, Thr75, Asn87, Pro88, Gly121, Gly122, Tyr124, Gly126, Trp286, Ser293, Val294, Phe295, Arg296, Try337 and Gly342. The hydrogen

bond interaction of Tyr124 with ZINC000035596918 had a significant contribution in ligand binding with a loss of -3.06 and -1.56 Kcal/mol energy in MM-GBSA and MM-PBSA, respectively, upon mutation with alanine residue. Tyr337, Phe338 and Tyr341 also displayed significant binding contribution. Val294 and Phe295 displayed significant contributions in MM-GBSA (**Figure 6.6**).

6.3.11. Molecular dynamics

The protein ligand complexes were subjected to energy minimisation. The energy states of protein-ligand complexes of ZINC000013719534, ZINC000035551243 and ZINC000035596918 were found to be -193540, -193390 and -193610 to -289910, -289690 and -289840 Kcal/mol, respectively, which indicated that the energy minimisation protocol had substantially minimised the complexes. The temperature of 310.15 K was attained at 11, 7 and 6 ps and density of the system attained to 1 g/cm^3 at 40, 41 and 43 ps for protein-ligand complexes of ZINC000013719534, ZINC000035551243 and ZINC000035596918, respectively. A short MD simulation run of 200 ps was used to check the stability and accuracy of the MD run. These simulations attained a stable RMSD at 96, 100 and 132 ps for complexes of ZINC000013719534, ZINC000035551243 and ZINC000035596918 with AChE, respectively (**Figure S11 – S13** in appendix).

The average RMSD was found to be 1.956, 1.605, 1.715, 1.689 and 1.877 Å for AChE, complexes of AChE with ZINC000013719534, ZINC000035551243, ZINC000035596918 and donepezil, respectively. Thus, the apo-form displayed higher deviation than ligand-bound forms, while the lowest deviation was observed for ZINC000013719534. The RMSD of the three selected ligand complexes were lower than donepezil-protein complex, indicating better binding. Mean RMSD deviations of 1.073, 1.317, 0.884 and 1.315 Å were observed for ZINC000013719534, ZINC000035551243

ZINC000035596918 compounds and donepezil, respectively, when bound to the enzyme. Further, there was not much deviation between average RMSD and the RMSD at the end of the 50th ns in all the cases indicating the stability of protein-ligand complexes (**Figure 6.7**).

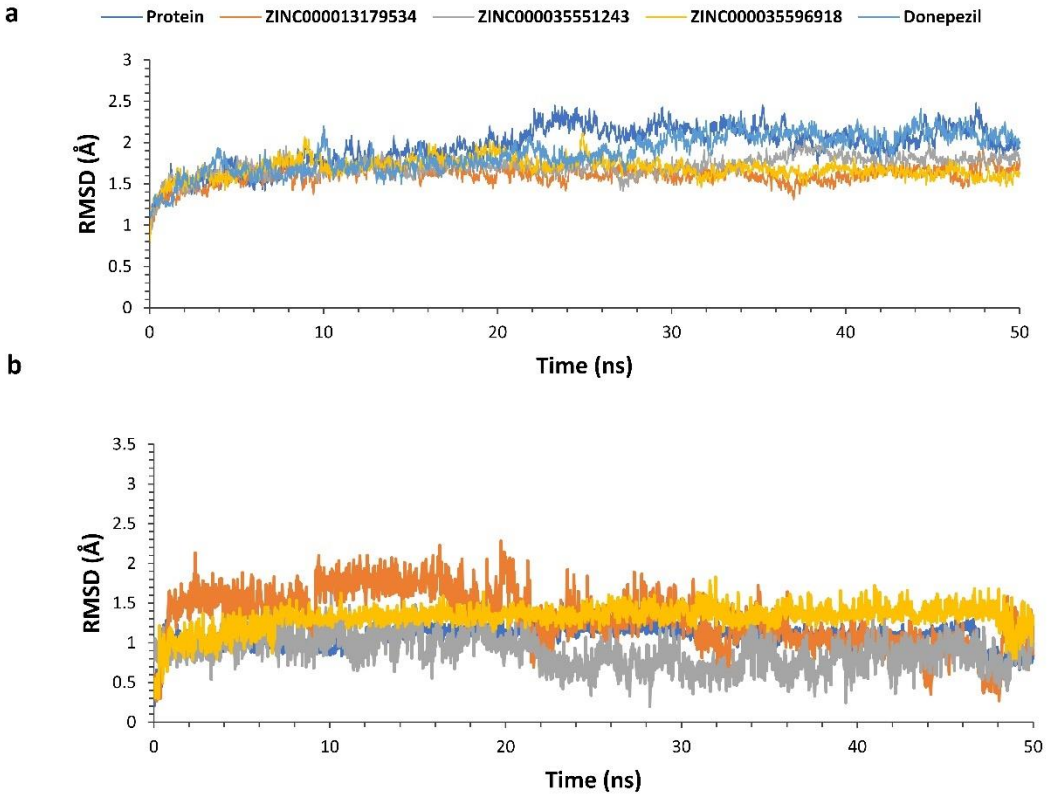

Figure 6.7 (a) RMSD plots of AChE protein backbone of apo-form, and complexed with ZINC000013719534, ZINC000035551243, ZINC000035551243, and donepezil (b) RMSD plots of ZINC000013719534, ZINC000035551243, ZINC000035551243, and donepezil bound to AChE.

The RMSF of protein-ZINC000013719534 complex displayed lower fluctuations with residues 65-86, 118-122, 285-298 and 331-339 than uninhibited enzyme. The residues 65-85 and118-122 formed van der Waals interactions with the ligand in the docking study (**Figure 6.8**). The amino acid residues Trp86, Tyr124 and Tyr337 displayed hydrogen bonding, while Trp286, Phe297, Phe338 and Tyr341 interacted through π-π and π-alkyl interactions. The docking study of protein-ZINC000035551243 complex displayed hydrogen bonding with Trp86 which was also indicated in RMSF plot through low fluctuation in comparison to uninhibited AChE enzyme. The other hydrogen bond was

formed by Ser125 residue that also displayed a similar RMSF pattern. The regions of 283-298 and 331-342 displayed π-π and π-alkyl interactions with ZINC000035551243 in docking study. This was also reflected through a lower RMSF of the correspondimg residues in the MD study.

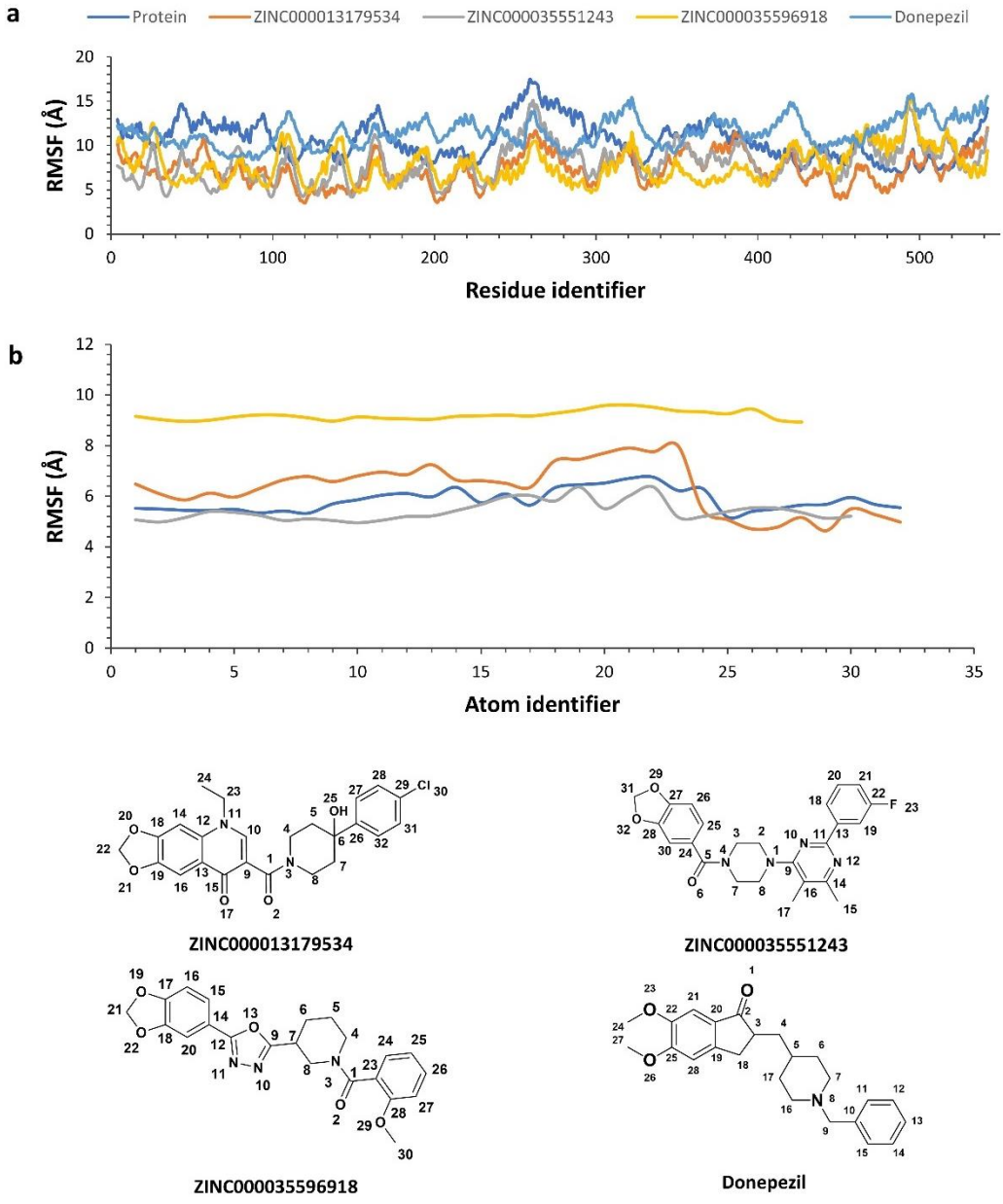

Figure 6.8 (a) RMSF plot of protein residue fluctuations of AChE apo-form and complexed with ZINC000013719534, ZINC000035551243, ZINC000035551243, and donepezil (b) RMSF plot of ZINC000013719534, ZINC000035551243, ZINC000035551243, and donepezil atoms.

ZINC000035596918 interacted with Gly121, Gly122 and Tyr124 through hydrogen bonds, leading to their subsequent stabilisation observed in the RMSF fluctuations. The residues Glu292 and Phe295 also formed hydrogen bonds, Val294, Tyr337, Phe338 and Tyr341 formed π- π and π-alkyl interaction with ligand resulting in stabilisation of protein in these regions. Further, the donepezil-AChE complex has displayed higher fluctuation than that of the selected ligands, which further highlighted that the three selected ligands outperformed donepezil in terms of binding stability.

The ligand RMSF indicated that the solvent-exposed regions of all ligands were less stable.The fused *benzo[d][1,3] dioxolyl* moiety had maximum RMSF deviation in ZINC000013719534, while in the case of ZINC000035551243 and ZINC000035596918 *para-fluoro phenyl* and *benzo[d][1,3]dioxolyl* moieties respectively had maximum RMSF. The *indene* moiety of donepezil also displayed fluctuation. The average SASA(s) for complete MD simulation were found to be 21703.23, 21392.96, 21318.78, 21582.27 and 21768.18 $Å^2$ for AChE, ZINC000013719534, ZINC000035551243 ZINC000035596918 and donepezil complexes of AChE, respectively. It was observed that there was a decrease in SASA values after ligand binding in the cases the three identified hits. This indicated that the selected ligands were binding in the tunnel around PAS resulting in decreased SASA (**Figure 6.9**).

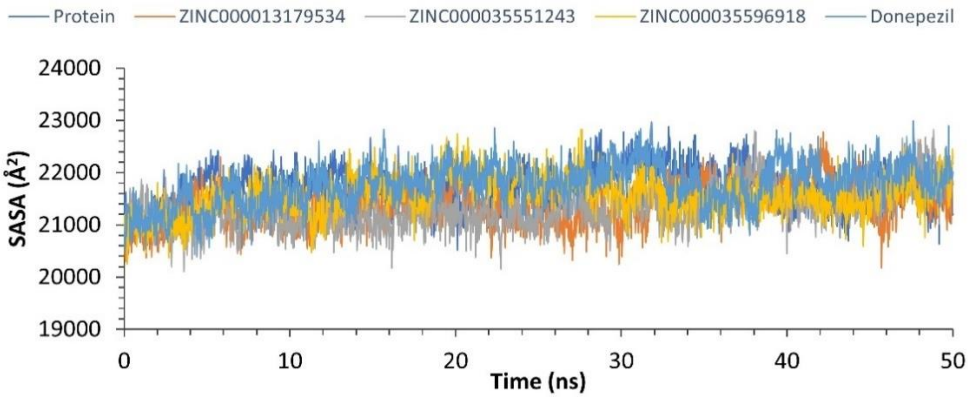

Figure 6.9 Solvent Accessible Surface Area, the plot of AChE (apo-form) and AChE complexed with ZINC000013719534, ZINC000035551243, ZINC000035551243, and donepezil.

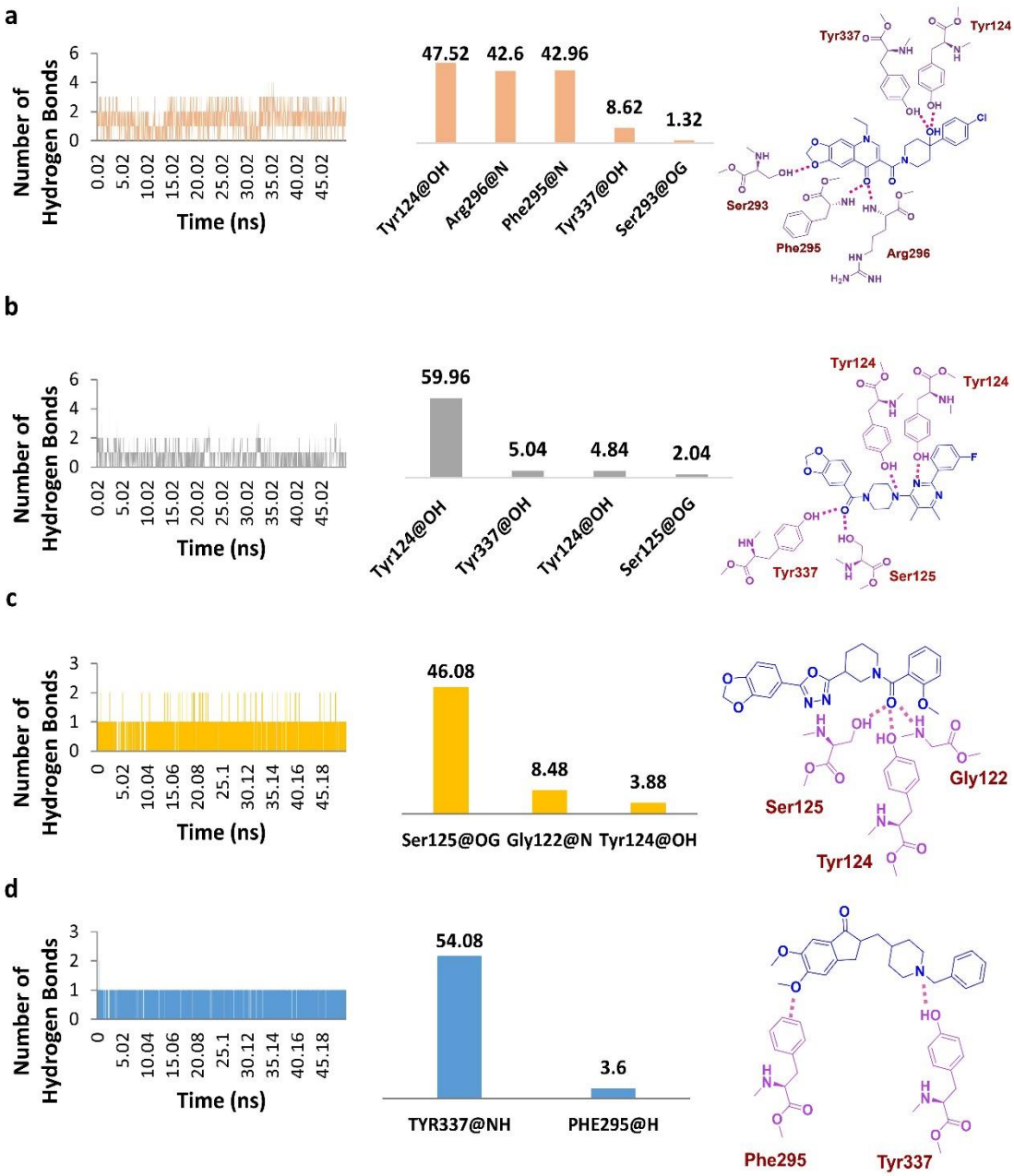

Figure 6.10 Hydrogen bond interaction analysis, critical residues and their contact time during hydrogen bond interactions of ZINC000013719534, ZINC000035551243, ZINC000035551243, and donepezil with protein during MD run.

ZINC000013719534 displayed hydrogen bond with Tyr124, Phe295 and Arg296 for 47.52, 42.96 and 42.6 % of the time during the simulation. ZINC000035551243 displayed hydrogen bonding for 59.96% of the time with Tyr124. The third compound ZINC000035596918 displayed hydrogen bonding with Ser125 for 48.06% of the time. Donepezil displayed hydrogen bonding with Tyr337 for 54.08% of the time. The study

highlighted that the crucial residues that were contributing protein-ligand stability through hydrogen bonding (**Figure 6.10**).